Vol. 45, No. 3 (2023) 522-531, DOI: 10.24874/ti.1503.06.23.08

Tribology in Industry

www.tribology.rs

RESEARCH

Role of Particle Shape on Slurry Erosion Wear of AA6063

Bhushan D. Nandre[a,b] and Girish R. Desale[a,*]

[a]*CSIR-National Chemical Laboratory, Dr. Homi Bhabha Road, Pune, Maharashtra, India,*
[b]*M.E.S.College of Engineering, Pune, Savitribai Phule Pune University, Maharashtra, India.*

Keywords:

Particle shape
Mild steel shots and grits
S.S. shots and grits
Kinetic energy

* Corresponding author:

Girish R. Desale
E-mail: gr.desale@ncl.res.in

Received: 27 June 2023
Revised: 18 July 2023
Accepted: 20 August 2023

A B S T R A C T

The shape of erodent particles is most critical parameter, which affects the material removal from the target surface. The effect of particle shape on slurry erosion is still under investigation. The kinetic energy of the impacting particle is, in principle, responsible for removal of material from the target surface, which is a function of particle size, shape, density and velocity. In the present work, the variation of the wear with particle size and shape has been analysed to establish relationship between the two. Also the effect of particle shape on the maximum wear and normal impact wear has been investigated. The variations of mass loss form AA6063 target material due to four different shapes of erodents, namely, mild steel shots, mild steel grits, S.S. shots and S.S. grits are determined at two orientation angles 45° and normal impact angle. The kinetic energy of impacting particles was kept constant during all experiments by varying other parameters like velocity of impacting particles, solid concentration and test duration. So the effect of impacting particle shape on erosion wear has been investigated with constant kinetic energy effect at 45° and 90° impact angles. The worn out surfaces have also been studied using SEM to understand the material removal mechanism.

1. INTRODUCTION

Solid particle erosion depends on characteristics of target material, solid particle material, carrier fluid, impact angle, impact velocity, and the particle size and shape. Hence, it is essential to understand the mechanisms of material removal due to erosion wear of the different parameters affecting it. Also spherical and angular particles show different material removal rate due to change in the wear mechanisms [1-6]. The commonly accepted erosion mechanisms are classified as Cutting, Ploughing, Extrusion and Forging and Subsurface deformation and cracking.

In fact, the shape of particle determines the contact area between the particle and the target surface during the impact. It is well known that the erosion by angular particles is

higher than that by the rounded particles. Levy and Chick [7] used angular steel grit and spherical steel shots for erosion of AISI 1020 steel. They observed that the erosion due to angular particles is around four times more than that due to the spherical particles. They attributed this phenomenon to formation of sharp craters by angular particles. Feng and Ball [8] reported that angular shape particles are significantly more erosive than rounded shape particles of the same size and mass. Also, the change in particle size and shape changes the particle contact area with the target surface and which further changes the stress concentration and affects the material removal rate. Hutchings [9] proposed two different mechanisms of material removal for spherical and angular particles. He proposed that the impact of round particles removes the target material by ploughing and displacing around the crater formed due to particles impact. Whereas, an angular particles removes the material from target surface by cutting mechanism due to forward or backward rotation of particles in the slurry.

The cutting and ploughing are commonly accepted erosion mechanisms which are mainly depend on the impacting particle shape as shown in Fig. 1. A highly deformed region is produced under the tip of impacting particle during cutting action (Fig. 1 (a)). The cutting wear dominates in case of angular particles whereas ploughing wear takes place for spherical particles. The cutting wear is also affected by the particle rotation Finnie [10]. Material removal by ploughing occurs when a spherical particle impacts on the target surface at large negative rake angle, causing surface shearing and displacing the material as shown in Fig. 1 (b). Thus the role of rake angle is decisive to cause the wear by cutting or ploughing. Generally, rake angle larger than 60° produces chips and show cutting type wear whereas at smaller rake angles, the material removal takes place by ploughing in the direction of particle impact [11]. The shape of solid particle can be described by different parameters like sphericity, aspect ratio, shape factor etc. [12-13].

The term sphericity (ϕ) is used to represent the closeness of the particle shape to a sphere. For spherical particles, the sphericity is equal to one. The term aspect ratio is defined as the ratio of the length of minor to major axis of the particle. This factor only reflects the elongation of the particle, but it does not make a distinction between square and circle. Another most important term known as shape factor which also known as circularity. Cox [1927] has defined a shape factor based on the projected area of the particle (A) and the overall perimeter of the projection (P) as under,

$$\textit{Shape factor, S.F.} = \frac{4\pi A}{P^2} \tag{1}$$

Accordingly, in the present investigation shape factor has been determined of spherical and angular solid particles made of mild steel and stainless steel. Afterwards the effect of shape of particles is correlated with the mass removal from AA 6063 target material.

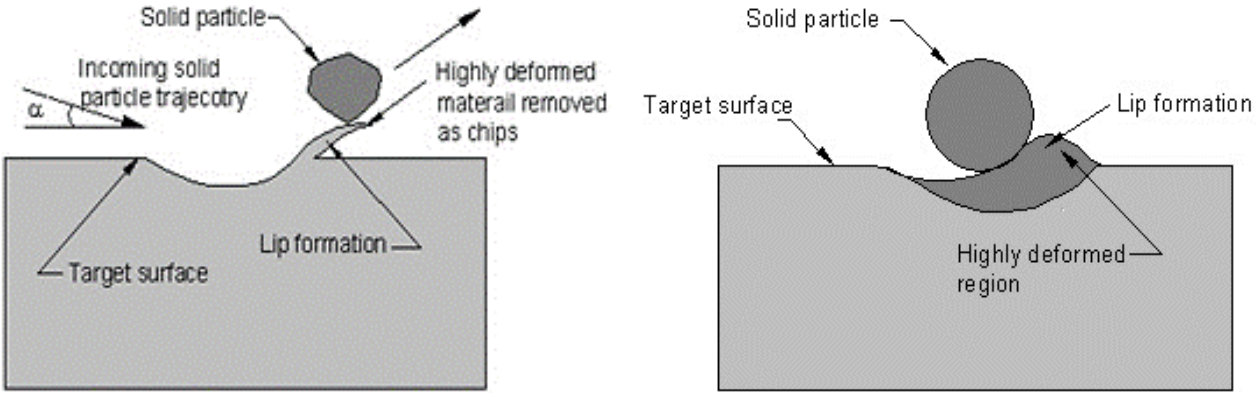

(a) Cutting mechanism by an angular particles

(b) Ploughing mechanism by spherical particles

Fig. 1. Material removal mechanism for different shapes of particles [7].

2. PROPERTIES OF MATERIALS USE

In the present investigation aluminium alloy 6063 (AA 6063) is used as target material and its chemical composition is given in Table 1. The hardness of AA 6063 is observed around 91 Hv.

The solid particles of mild steel and stainless steel having spherical and angular shapes with four different sizes 256 μm, 362.5 μm, 462.5 μm and 550 μm are used to form solid-liquid mixtures with tap water to conduct experiments on erosion wear. The physical properties of solid particles are given in Table 2.

The shape of solid particles is difficult to define and quantify for the irregular shape of erodents. However, the attempts have been made to calculate the shape factor of each erodent by examining the micrographs of erodents [14]. Scanning electron microscope (SEM) images of all four solid particles with 362.5 μm size are presented in Fig. 2 (a-d). It is observed that the particle shape of all four erodents is different. It is observed from Fig. 2 (a-d) that mild steel particles having completely spherical shape compared to S.S. particles of globular shape. However, M.S. angular particles are having more angularity with cutting edges compared to S.S. angular particles.

Table 1. Chemical composition of target material (AA 6063).

Element	Cu	Fe	Zn	Mn	Si	Cr	Mg	Ti	Al
Content (%)	0.013	0.24	0.01	0.055	0.389	0.015	0.510	0.008	Balance (98.76)

Table 2. Physical properties of erodent used*Supplier data.

Sr. No.	Solid Particle	Colour*	Density* (Kg/m^3)	Hardness* (Hv)	Particle Shape*	Shape factor
1	M.S. spherical particles	Blackish	7600	400	Spherical	1.0
2	M.S. angular particles			600	Angular	0.3425
3	S.S. spherical particles	Silver grey	7860	300	Spherical/ globular	0.9
4	S.S. angular particles			700	Angular	0.4425

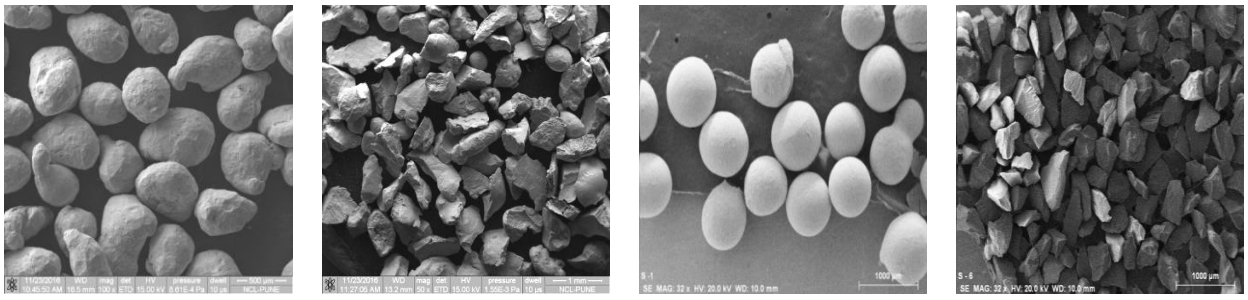

(a) S.S. Shots (b) S.S. Grits (c) M.S. shots (d) M.S. Grits

Fig. 2. SEM images of erodents of size 362.5 μm.

A shape factor has been determined for all four erodent particles using equation 1. The SEM micrographs of all solid particles were analysed with Axio Vision 4.1 analyser. The area (pixel^2) and perimeter (pixel) of an individual particle are measured and used to evaluate the shape factor. It is observed that the shape factor is 1 for M.S. spherical particles, whereas, it is 0.9, 0.4425 and 0.3425 for S.S. spherical, S.S. angular and M.S. angular particles, respectively. The hardness and shape factor of all erodents are given in Fig. 3.

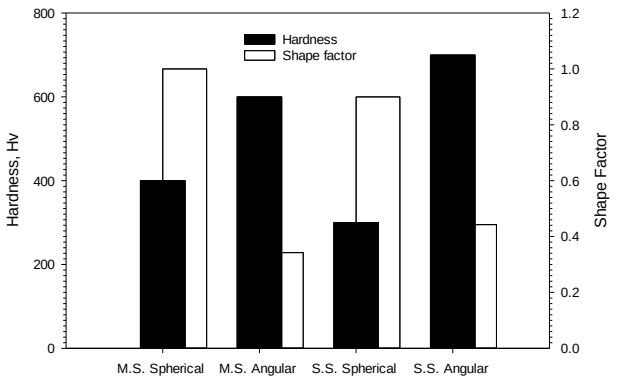

Fig. 3. Hardness and shape factor of different erodents.

3. EXPERIMENTAL PROGRAM

In the present investigation, slurry pot tester has been used to conduct erosion wear experiments [15,16]. In the present experimental study, two different shapes spherical and angular of mild steel and stainless steel particles having four different sizes 256 μm, 362.5 μm, 462.5 μm and 550 μm were used to form solid-liquid mixture. Total numbers of impacting particles and kinetic energy during all the experiments were kept constant by varying operating parameters like velocity of impacting particles, solid concentration and test duration as given in Table 3. The fixture was mounted on the indexing plate in the slot of 45° and 90° impact angle for desired test duration as given in Table 3 to maintain the constant number of striking particles and thus kinetic energy.

Initially, 550 μm size mild steel particles with 30 % by wt. solid concentration impacted with 2.23 m/s velocity on AA6063 target material for 60 min test duration. The kinetic energy of the individual particles was determined around 1.64×10^{-7} J using the equation 2. To maintain this individual particle kinetic energy for remaining particle sizes, the velocity is varied from 2.23 to 7.02 m/s as given in Table 3.

$$K.E.(single\ particle) = \frac{2}{3}\pi r^3 \rho V^2 \quad (2)$$

Where, r, ρ, V are radius, density and velocity of impacting particle, respectively.

The 30 % by wt. solid concentration determines 2.92 kg mild steel particles in the slurry. Accordingly, total numbers of particle striking on the target surface during experiment were around 710637779. Thus, the total kinetic energy imparted on the target material is around 1169 J. To maintain overall constant kinetic energy of M.S. spherical particles with other three particle sizes, the % wt. solid concentration is varied from 3.02 to 30 % by wt. as given in Table 3.

The numbers of striking particles are different for 45° and 90° impact angle due to different swept volume. [17]. Thus, to maintain the constant kinetic energy at both impact angles for M.S. particles the test duration is varied accordingly from 13.4 min to 60.0 min (Table 3).

However, S.S. particles having different density than M. S. particles therefore it changes the individual solid particle mass and kinetic energy. Therefore, for S.S particles, to maintain the constant kinetic energy 1.64×10^{-7} J, the velocity is varied from 2.19 to 6.90 m/s (Table 3). Additionally, to maintain the overall constant kinetic energy of S.S. particles the % by wt. solid concentration is varied from 3.2 to 31.74 % by wt. as given in Table 3. Also, to maintain constant kinetic energy for 45° and 90° impact angles the test duration of S.S. particles is varied from 13.6 to 61.9 min (Table 3).

Thus, the kinetic energy of individual particle of all types of erodents is maintained constant during all experimental conditions by varying the other parameters as given in Table 3.

Table 3. Range of parameters.

Erodents used	Particle size (μm)	Average mass of individual particle (x 10^{-7}), kg	Solid concentration % by wt. (Cw)	Velocity of particle (m/s)	Impact angle	Test duration (min)
M.S. particles	550	6.61	30	2.23	45°	60.0
					90°	42.4
	462.5	3.93	17.83	2.89	45°	46.2
					90°	32.7
	362.5	1.89	8.58	4.16	45°	32.1
					90°	22.6
	256	0.667	3.02	7.02	45°	19.0
					90°	13.4
S.S. particles	550	6.84	31.74	2.19	45°	61.9
					90°	43.7
	462.5	4.06	18.87	2.84	45°	47.0
					90°	33.2
	362.5	0.195	9.08	4.09	45°	32.6
					90°	23.0
	256	0.690	3.2	6.90	45°	19.3
					90°	13.6

4. RESULTS AND DISCUSSION

The erosion wear behaviour of AA 6063 target material using spherical and angular shape particles of M.S. and S.S. at constant kinetic energy is investigated. The variation in mass loss per particle from the AA 6063 target material surface for respective experimental conditions due to spherical and angular shapes of M.S. and S.S. erodents is given in Table 4.

4.1 Effect of particle shape

The kinetic energy and the total number of impacting particles were kept constant to determine the mass loss from the target material surface (AA6063) at 45° and 90° orientation angles. The mass loss per particle is calculated by dividing the total mass loss from target surface with total number of particles striking the surface during experiment. The variation in mass loss per particle with particle shape factor is graphically presented in Fig. 4 for 45° and 90° impact angles, respectively. It is observed that the target material AA 6063 shows different mass loss per particle due to impact of four different erodents, though the particles dissipates same constant kinetic energy at target surface. It is observed from Fig. 4 (a and b) that the angular particles of both mild steel and stainless steel show higher mass loss (material removal) from target surface compare to spherical shape particles at both impact angles. It is also observed that increasing the shape factor (roundness) of solid particles decreases the erosion wear. These results are in well agreement with the findings reported by many investigators in this field [18-22]. They have reported that the angular shape particles are significantly more erosive than rounded shape particles of the same size and mass.

Table 4. Range of parameters and observed mass loss, Number of particles in pot=710637779, Kinetic energy of individual particle= 1.64 x 10^{-7} J, Total kinetic energy of the impacting particles on the specimen= 1169 J.

Erodents used	Particle Size (μm)	Solid concentration % by weight (Cw)	Velocity of particle (m/s)	Impact angle	Test Duration (min)	Mass loss per particle (x 10^{-12}), g
M.S. Shots	550	30	2.23	45°	60.0	6.47
				90°	42.4	3.86
	462.5	17.83	2.89	45°	46.2	6.40
				90°	32.7	3.72
	362.5	8.58	4.16	45°	32.1	6.19
				90°	22.6	3.72
	256	3.02	7.02	45°	19.0	5.91
				90°	13.4	3.51
M.S. Grits	550	30	2.23	45°	60.0	9.85
				90°	42.4	5.76
	462.5	17.83	2.89	45°	46.2	9.56
				90°	32.7	5.62
	362.5	8.58	4.16	45°	32.1	9.28
				90°	22.6	5.34
	256	3.02	7.02	45°	19.0	9.00
				90°	13.4	5.20
S.S. Shots	550	31.74	2.19	45°	61.9	6.54
				90°	43.7	3.94
	462.5	18.87	2.84	45°	47.0	6.33
				90°	33.2	3.79
	362.5	9.08	4.09	45°	32.6	6.19
				90°	23.0	3.72
	256	3.2	6.90	45°	19.3	6.05
				90°	13.6	3.65
S.S. Grits	550	31.74	2.19	45°	61.9	9.99
				90°	43.7	5.76
	462.5	18.87	2.84	45°	47.0	9.50
				90°	33.2	5.56
	362.5	9.08	4.09	45°	32.6	9.14
				90°	23.0	5.26
	256	3.2	6.90	45°	19.3	8.72
				90°	13.6	5.06

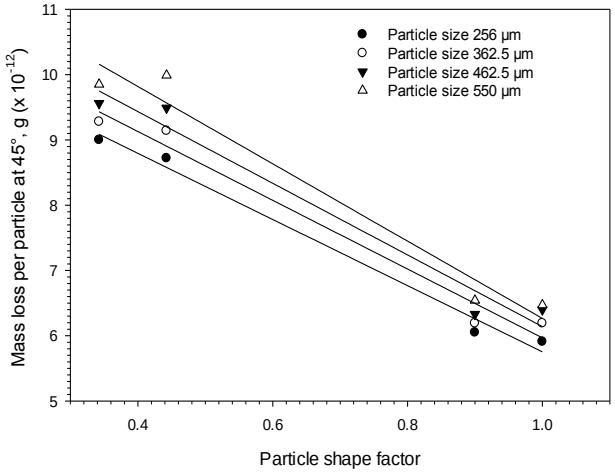

(a) At 45° impact angle

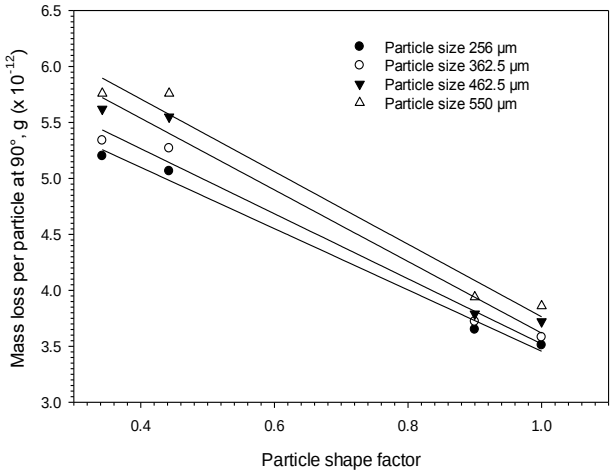

(b) At 90° impact angle

Fig. 4. Variation in mass loss per particle from AA6063 target specimen with shape factors of erodents (M.S. and S.S.) impacting with constant kinetic energy.

The effective radius (Re) of angular particles may be less as compare to spherical particle as shown in Fig. 5.

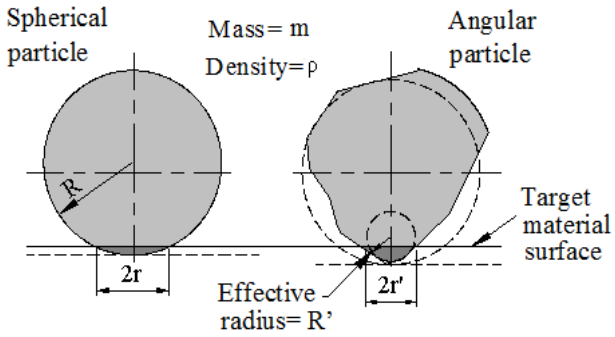

Fig. 5. Contact area of spherical and angular erodent with flat surface [23].

It is also observed that the minor variation in the mass loss is observed due to the spherical shape M.S. and S.S. particles which can be attributed to the small variation in shape and hardness of erodent materials. While, with the angular particle of M.S. shows little higher wear compare to the harder S.S. particles. This reveals that the angularity of erodent plays dominant role than its hardness beyond a certain value, which is in line with the results reported by many investigators [24-26].

4.2 Effect of particle size

It is reported by many investigators that erosion wear increases with particle size [27-29]. However, the variation in erosion wear occurs for same size particles due to uneven shape of particle. Accordingly, in the present study, the effect of particle size and shape is re-examined with the solid particles of spherical and angular shapes of M.S. and S.S. impacting with constant kinetic energy.

The mass loss data given in Tables 4 is again used to understand its variation with the particle size and graphically presented in Fig. 6 (a and b) for 45° and 90° impact angles. It is observed from Fig. 6 (a and b) that the mass loss per particle sluggishly increases with increasing the particle size for both spherical and angular shape at both 45° and 90° impact angles. The smaller mass loss incremental value corresponds to the incremental value of particle size. This smaller mass loss incremental can be attributed to different solid loading, striking efficiency and different contact area for different particle sizes. It reveals that the mass loss due to impact of solid particles is a strong function of kinetic energy irrespective of its size.

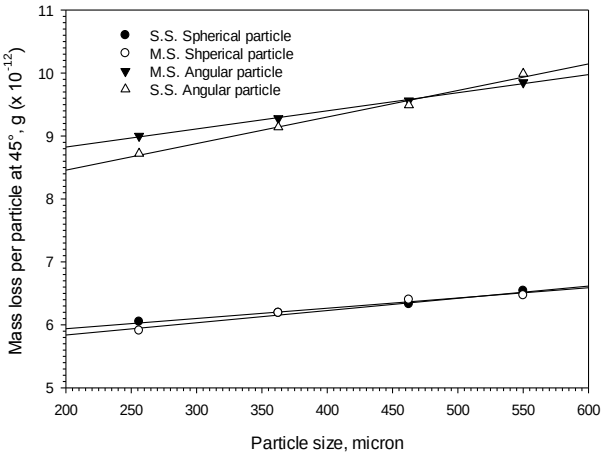

(a) At 45° impact angle

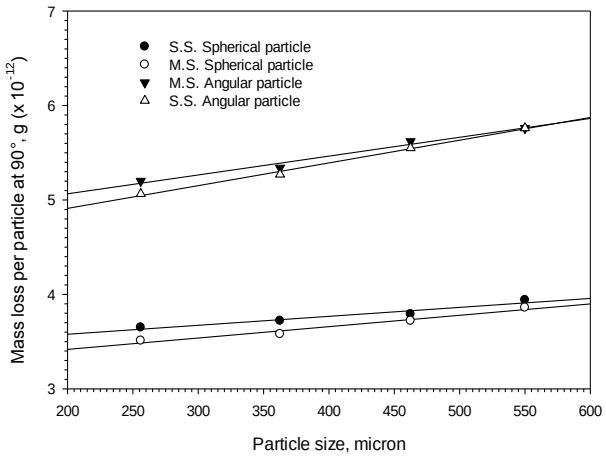

(b) At 90° impact angle

Fig. 6. Variation in mass loss per particle from AA6063 target specimen with different impacting particle size at constant kinetic energy.

5. SEM EXAMINATION

The SEM images of worn out specimens of AA6063 target material due to impact of 362.5 μm size of M.S. and S.S. spherical and angular shape of erodent are presented for 45° impact angle in Fig. 7 (a-d) while for 90° impact angle are presented in Fig. 8 (a-d).

The ploughing type craters are observed on test specimen due to impact of spherical shape mild steel and S.S. particles in the direction of flow as shown in Fig. 7 (a-b). However, the micro-cutting material removal mechanism (Fig. 7 (c and d)) is observed due to impact of angular shape of mild steel and S.S. particles.

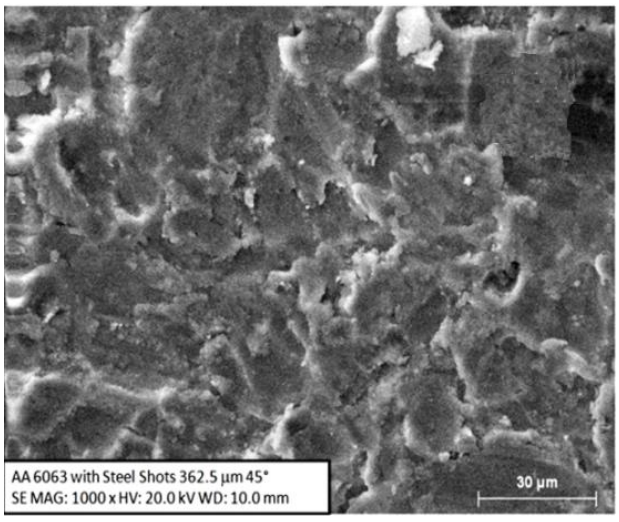

(a) Spherical shape M.S. particles

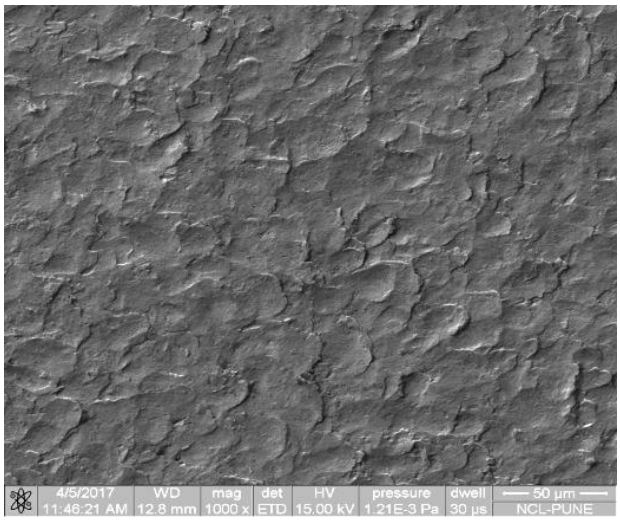

(b) Spherical shape S.S. particles

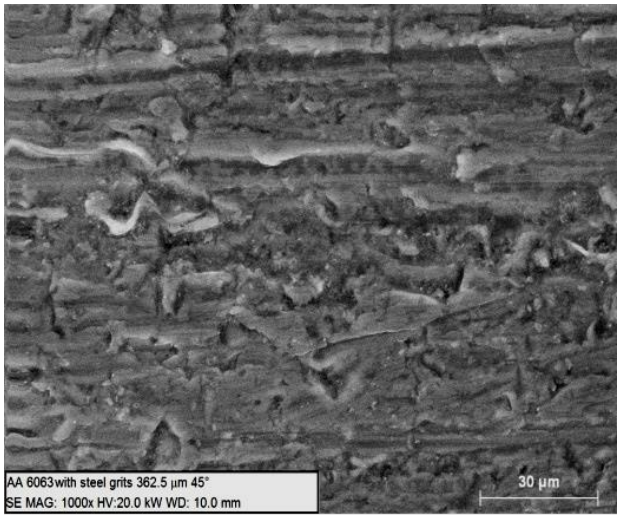

(c) Angular shape M.S. particles

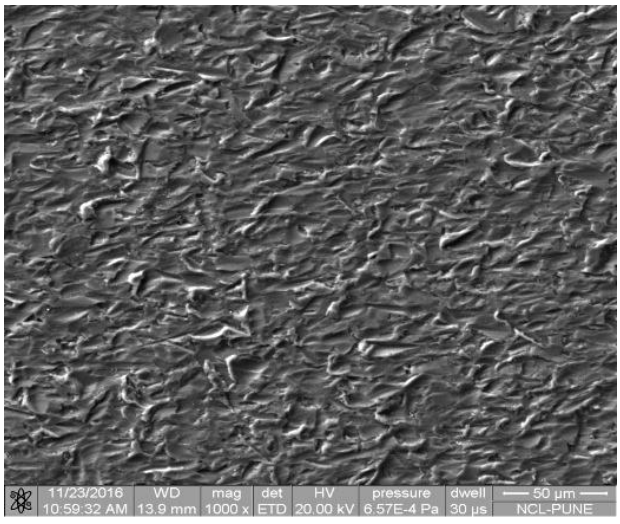

(d) Angular shape S.S. particles

Fig. 7. (a-d) SEM images of worn out surfaces of AA6063 due to impact of spherical and angular shape of M.S. and S.S. particles at 45° impact angle (Particle size 362.5 μm)

Also, it is observed that the crater geometries are different for the different erodents. The craters formed due to impact of angular erodents are longer in length, and less in width compare to spherical shape mild steel and S.S. particles. This reveals that the angular shape particles effectively remove more material by cutting action rather than ploughing. This also gives evidence that cutting mechanism removes the material more effectively than ploughing.

Similarly, it is observed from Fig. 8 (a-d) that the wear due to deformation is dominant at normal impact angles. The spherical shape particles are responsible to form indentation craters with circular rim on the eroded surface (see Fig. 8 (a-b)). The successive impact of spherical particles may flattened the rim and responsible for removal of material in the form of chip. While, due to angular particles at normal impact, the size of the craters becomes smaller and uneven (see Fig. 8 (c-d)), thus the stress concentration on the surface may be more compare to the spherical shape particles.

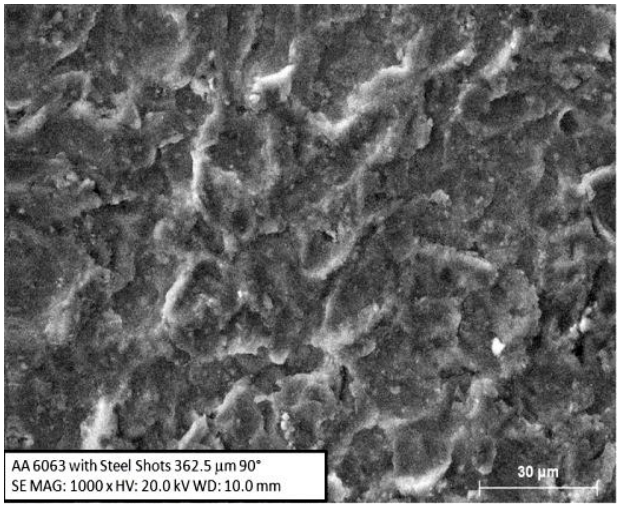

(a) Spherical shape M.S. particles

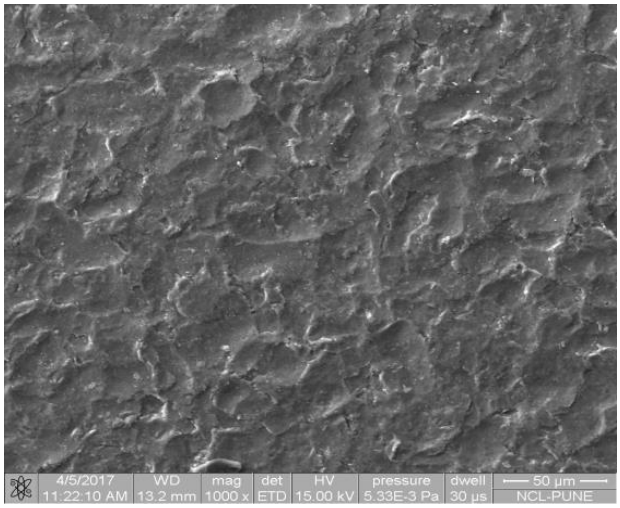

(b) Spherical shape S.S. particles

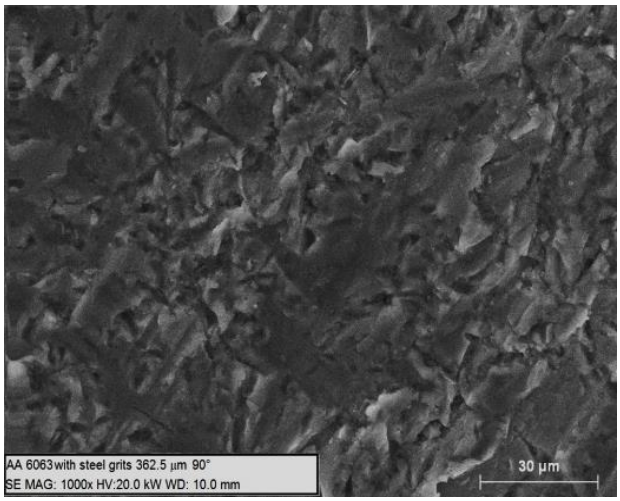

(c) Angular shape M.S. particles

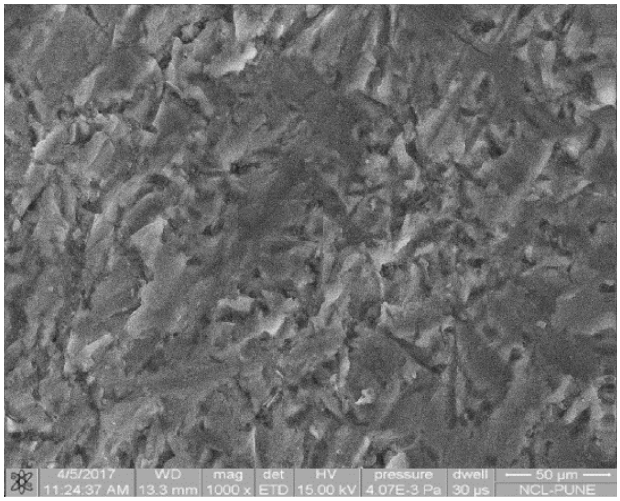

(d) Angular S.S. particles

Fig. 8. (a-d) SEM images of worn out surfaces of AA6063 due to impact of spherical and angular shape of M.S. and S.S. particles at 90° impact angle (Particle size 362.5 µm).

6. CONCLUSION

The effect of particle shape on erosion wear of AA 6063 is investigated using two different erodents namely, mild steel and S.S. having spherical and angular shapes. Four different particle sizes (256 µm, 362.5 µm, 462.5 µm and 550 µm) with constant kinetic energy are impacted at 45° and 90° impact angles. Based on the experimental results the following conclusions are drawn:

1. Though the kinetic energy of all erodent was kept constant, the angular shape of mild steel and S.S. particles are responsible for more material loss from target surface compared to spherical shape particles at both orientation angles. Thus, apart from the kinetic energy of impacting particle its shape also plays key role in material removal mechanism from the target surface.

2. The constant kinetic energy of different size particles is responsible for almost constant mass loss per particle for all erodents at both orientation angles. It reveals that kinetic energy play its important role irrespective of its size of particles.
3. However, at 45° impact angle all the four erodents effectively remove more material from the target surface compare to normal impact angle. This reveals that all shapes of erodents effectively remove more material at acute impact angle compare to normal impact due to different material removal mechanism at both impact angles.
4. The different material removal mechanism observed for different particle shape and impact angle. Solid particles having lower shape factor, produces deep craters and higher stress concentration compare to the particles having higher shape factor. At shallow impact angles the material is removed due to cutting action from the target surface. While at normal impact angle, the material is removed due to plastic deformation. Thus, the erosion rate by angular particles at shallow impact angle is significantly high.

Acknowledgment

The authors gratefully acknowledge the financial support from CSIR-NCL Pune and are thankful to Dr. Ashish Lele Director, Pune.

REFERENCES

[1] I.M. Hutchings, R.E. Winter, *Particle erosion of ductile metals: A mechanism of material removal*, Wear, vol. 27, iss. 1, pp. 121-128, 1974, doi: 10.1016/0043-1648(74)90091-X

[2] I.M. Hutchings, *Mechanism of the erosion of metals by solid particles*, in W.F. Adler (Ed.), Erosion: Prevention and useful Applications, ASTM STP 664, ASTM, pp. 59-76, 1979.

[3] I.M. Hutchings, R.E. Winter, *The erosion of ductile metals by spherical particles*, Journal of Physics D: Applied Physics, vol. 8, pp. 8-17, 1975, doi: 10.1088/0022-3727/8/1/010

[4] S.R. More, D.V. Bhatt, J.V. Menghani, *Study of the Parametric Performance of Solid Particle Erosion Wear under the slurry Pot Test Rig*, Tribology in Industry, vol. 39, no. 4, pp. 471-481, 2017, doi: 10.24874/ti.2017.39.04.06

[5] C.I. Walker, M. Hambe, *Influence of particle shape on slurry wear of white iron*, Wear, vol. 332-333, pp. 1021-1027, 2015, doi: 10.1016/j.wear.2014.12.029

[6] M. Liebhard, A. Levy, *The effect of erodent particle characteristics on the erosion of metals*, Wear, vol. 151, iss. 2, pp. 381-390, 1991, doi: 10.1016/0043-1648(91)90263-T

[7] A.V. Levy, P. Chik, *The effects of erodent composition and shape on the erosion of steel,* Wear, vol. 89, iss. 2, pp. 151-162, 1983, doi: 10.1016/0043-1648(83)90240-5

[8] Z. Feng, A. Ball, *The erosion of four materials using seven erodents—towards an understanding*, Wear, vol. 233–235, pp. 674–684, 1999, doi: 10.1016/S0043-1648(99)00176-3

[9] I.M. Hutchings, *A model for the erosion of metals by spherical particles at normal incidence*, Wear, vol. 70, iss. 3, pp. 269-281, 1981, doi: 10.1016/0043-1648(81)90347-1

[10] I. Finnie, *Some observations on the erosion of ductile metals*, Wear, vol. 19, iss. 1, pp. 81-89, 1972, doi: 10.1016/0043-1648(72)90444-9

[11] I.M. Hutchings, *Energy absorbed by elastic waves during plastic impact*, Journal of Physics D: Applied Physics, vol. 12, no. 11, pp. 1819-1824, 1979, doi: 10.1088/0022-3727/12/11/010

[12] S. Bahadur, R. Badruddin, *Erodent particle characterization and the effect of particle size and shape on erosion*, Wear, vol. 138, iss. 1-2, pp. 189-208, 1990, doi: 10.1016/0043-1648(90)90176-B

[13] R. Bellman Jr., A. Levy, *Erosion mechanism in ductile metals*, Wear, vol. 70, iss. 1, pp. 1-27, 1981, doi: 10.1016/0043-1648(81)90268-4

[14] G.R. Desale, B.K. Gandhi, S.C. Jain, *Effect of erodent properties on erosion wear of ductile type materials*, Wear, vol. 261, iss. 7-8, pp. 914–921, 2006, doi: 10.1016/j.wear.2006.01.035

[15] G.R. Desale, B.K. Gandhi , S.C. Jain, *Improvement in the design of a pot tester to simulate erosion wear due to solid–liquid mixture*, Wear, vol. 259, iss. 1-6, pp. 196–202, 2005, doi: 10.1016/j.wear.2005.02.068

[16] G. Desale, *Study on Slurry Erosion Behavior of Ductile Type Material and Laser Cladded Surface*, PhD thesis, Indian Institute of Technology, Rurckee, India, 2006.

[17] B.D. Nandre, G.R. Desale, *The Effects of Constant Kinetic Energy of Different Impacting Particles on Slurry Erosion Wear of AA 6063*, Journal of Tribology, vol. 140, iss. 3, pp. 1-8, 2018, doi: 10.1115/1.4038355

[18] J.B. Zu, I.M. Hutchings, G.T. Burstein, *Design of slurry erosion test rig*, Wear, vol. 140, iss. 2, pp. 331-344, 1990, doi: 10.1016/0043-1648(90)90093-P

[19] F.Y. Lin, H.S. Shao, *Effect of impact velocity on slurry erosion and a new design of a slurry erosion tester*, Wear, vol. 143, iss. 2, pp. 231-240, 1991, doi: 10.1016/0043-1648(91)90098-F

[20] H.McI. Clark, *On the impact rate and impact energy of particles in a slurry pot erosion tester*, Wear, vol. 147, iss. 1, pp. 165-183, 1991, doi: 10.1016/0043-1648(91)90127-G

[21] R. Gupta, S.N. Singh, V. Seshadri, *Prediction of uneven wear in a slurry pipeline on the basis of measurements in a pot tester*, Wear, vol. 184, iss. 2, pp. 169–178 1995, doi: 10.1016/0043-1648(94)06566-7

[22] B.K. Gandhi, S.N. Singh, V. Seshadri, *Study of the parametric dependence of erosion wear for the parallel flow of solid-liquid mixtures*, Tribology International, vol. 32, iss. 5, pp. 275-282, 1999, doi: 10.1016/S0301-679X(99)00047-X

[23] G.R. Desale, B.K. Gandhi, S.C. Jain, *Slurry erosion of ductile materials under normal impact condition*, Wear, vol. 264, iss. 3-4, pp. 322–330, 2008, doi: 10.1016/j.wear.2007.03.022

[24] A. Elkholy, *Prediction of abrasion wear for slurry pump materials*, Wear, vol. 84, iss. 1, pp. 39–49, 1983, doi: 10.1016/0043-1648(83)90117-5

[25] G. Sundararajan, P.G. Shewmon, *A new model for the erosion of metals at normal incidence*, Wear, vol. 84, iss. 2, pp. 237–258, 1983, doi: 10.1016/0043-1648(83)90266-1

[26] V. Javaheri, D. Porter, V.-T. Kuokkala, *Slurry erosion of steel-Review of tests, mechanism and materials*, Wear, vol. 408-409, pp. 248-273, 2018, doi: 10.1016/j.wear.2018.05.010

[27] H.M. Clark, *Specimen Diameter, Impact Velocity, Erosion Rate and Density in a Slurry Pot Erosion Tester*, Wear, vol. 162–164, pp. 669–678, 1993, doi: 10.1016/0043-1648(93)90065-T

[28] H.M. Clark, R.B. Hartwich, *A Re-Examination of the Particle Size Effect' in Slurry Erosion*, Wear, vol. 248, iss. 1–2, pp. 147–161, 2001, doi: 10.1016/S0043-1648(00)00556-1

[29] R.S. Lynn, K.K. Wong, H.M. Clark, *On the Particle Size Effect in Slurry Erosion*, Wear, vol. 149, iss. 1–2, pp. 55–71, 1991, doi: 10.1016/0043-1648(91)90364-Z